# CHAPTER 1. INTRODUCTION

## 1.1 Nonlinear dynamics in electrochemistry

In the last two decades, a great deal of mastery has been achieved that allows oscillatory reactions to be designed at will. This thesis introduces a variety of nonlinear electrochemical behaviours such as spontaneous oscillation of current or potential, complex spatiotemporal patterns of interfacial potential and associated bifurcation scenarios in the electrocatalytic oxidation of $C_1$ molecules.

The dynamic interplay of chemical reactions and electrical effects is a quite widespread feature. Not only is it the realm of electrochemistry, but it also occurs at biological membranes, most prominently in nerve cells and cardiac tissue. A large variety of spatiotemporal patterns have been observed in such systems, including accelerating or decelerating fronts, remote triggering, travelling pulses, standing waves, spirals and turbulence.

The occurrence of oscillations and pattern formation in electrochemistry has been known for a long time. In fact, electrochemistry is the oldest area in science where manifestations of nonlinear dynamics were found, since spontaneous oscillations were already observed in the early 19th century [1, 2]. Early model systems studied were the electrochemical dissolution of metals [3 – 8], and it became apparent that the observed oscillations were often accompanied or even caused by pulse propagation in the potential drop between electrode and electrolyte, since the optical observation of the simultaneous removal and consequent formation of an oxide film on the electrode was easily possible. This presumably marks the first attempt to establish a relation between physiological and physico-chemical rhythms [6]. It was also considered as a model of the protoplasmic or nerves type of transmission [5].

A renewed interest in electrochemical pattern formation has been seen after Wojtowicz [9] first summarised temporal electrochemical oscillations. Early research on spatial pattern formation remained generally scarce with a few studies focusing on metal dissolution or metal passivation where the observation of patterns was straightforward

[10, 11]. Starting from the observation of travelling pulses of current density in the electro-dissolution of nickel wires in acidic media [12], mainly fronts or pulse propagation and inhomogeneous oscillations [12 – 18] were studied. As a result of the development of micro-probe electrodes and surface plasmon microscopy [19] it became possible to extend the spatial investigation to electrocatalytic reactions like the oxidation of hydrogen, formic acid and methanol or the reduction of peroxodisulphate. Detailed experimental and theoretical investigations have shown a vast diversity of patterns, ranging from fronts [19 – 21], standing waves [22, 23], pulses [23] and complex oscillations [24] to various stationary inhomogeneous structures [25].

Since oscillations seemed to be in contradiction to (equilibrium) thermodynamics, periodic phenomena in chemistry were not accepted as reality or considered as curiosities through the 19th and until late last century. The introduction of non-equilibrium thermodynamics [26] and the concept of dissipation could explain this dilemma. When maintained far from equilibrium and open to exchange of energy and/or matter with their surroundings, nonlinear chemical systems can self-organise taking on ordered states of locally decreased entropy such as temporally periodic, chaotic or spatially periodic variations of concentrations of chemical species. Simultaneously, enhanced dissipation of energy through the system to the surroundings assures a net increase of entropy in accordance with the second law of thermodynamics. Stopping the exchange of energy and matter, the system gradually approaches chemical equilibrium until all patterns cease. Thus, the frequent observations of pattern formation and oscillations in electrochemistry is not surprising, since electrochemical kinetics is inherently nonlinear, and electrochemical experiments are usually carried out by imposing external constraints (*e.g.*, applying a constant potential drop between two electrodes) to create a far from equilibrium condition. This is one reason why so many self-organising electrochemical systems have been found until now. As will be discussed in this thesis, these inhomogeneous potential structures can be understood through a combination of nonlinear chemical reactions at the electrode and spatial coupling *via* ion migration. It can be described by an integral reaction-migration equation developed by Christoph [27].

# 1.2 Electrochemical instability and migration coupling

For a better understanding of spatiotemporal pattern formation in the electrocatalytic oxidation of $C_1$ molecules and the occurrence of spontaneous oscillations in physico-chemical systems, the following mathematical descriptions and theoretical basics of dynamical systems are indispensable. First of all, we should accurately define the terms variable and parameter. A parameter is a quantity to be controlled by the experimentalist, the value of which can be changed at will. Examples are the externally applied potential, temperature, bulk concentration and solution pH. A variable is a quantity that is chosen by the system and is usually a time-dependent quantity. Note that the current is not a variable but a parameter under galvanostatic conditions.

**Instability criteria**

Stable state means that the system is insensitive to small fluctuations. If a small perturbation takes the system away from the steady state, the system will return to the stable state after the perturbation has ceased. Thus, instability implies that any fluctuation, no matter how small, will make the system leave the steady state. Therefore, an unstable state can never be observed experimentally. Apart from the steady state, another state is the oscillatory state. An oscillatory state can also be stable or unstable, in the sense that it recovers from small fluctuations or not. In general, spontaneous oscillations in a physico-chemical system are related to the fact that the stationary state is unstable. Therefore, the question of why stable spontaneous oscillations occur in a given system must always also involve the question of why the stationary state is not stable. The transition from a stable state to an unstable state is usually accompanied by a bifurcation. Hence, a bifurcation in a non-equilibrium system is very much like a phase transition in an equilibrium system: under the influence of a certain control parameter, the system changes qualitatively from one type to the other type. The analogy between the phase theory of equilibrium systems and the bifurcation theory of dynamical (non-equilibrium) systems is useful for a first grasp of the understanding of what bifurcation theory entails, but is not, of course, entirely accurate. One possible misconception is that in the equilibrium phase theory a metastable phase is sometimes considered unstable.

However, a metastable state is unstable only with respect to large fluctuations but is stable with respect to small fluctuations.

## Bifurcation theory and impedance spectroscopy

Nonlinear chemical reaction systems operated far from equilibrium can exhibit a rich variety of dynamical states other than a single stationary state. In what is called a bifurcation, the non-equilibrium system switches from one type of dynamics to a qualitatively different type. Three bifurcations are of particular importance in the classification of electrochemical oscillators. The simplest instability involves two coexisting stable steady states for a given set of control parameters (bistability). This transition between monostability and bistability is referred to as *saddle-node bifurcation*, and it gives rise to hysteresis behaviour in current-potential curves. Spontaneous oscillations in physico-chemical systems are generally related to the fact that the steady state becomes unstable in favour of a periodic orbit. The transition point is referred to as *Hopf bifurcation*. Finally, more complex bifurcation can lead to unstable periodic orbits and can result in complex chemical dynamics such as deterministic chaos [28]. The third bifurcation, the so-called *homoclinic bifurcation*, is global in nature and is not detectable with a linear stability analysis. Its existence is usually assessed from a numerical integration of the differential equations.

The idea of linearising the system's equations about a stationary reference state will appear familiar to many electrochemists. It lies at the heart of electrochemical impedance spectroscopy. If one experimentally determines the system's linearised response over a wide enough frequency range, one essentially has all the linear information of the system and, hence, it must be possible to make statements about the system's stability. In an impedance spectroscopy experiment, one drives the electrochemical systems by a small-amplitude sinusoidal voltage modulation superimposed on a constant potential, and measures the resulting small amplitude sinusoidal current oscillations. The amplitude and the phase shift of the current modulation with respect to the voltage modulation together determine the complex impedance of the system. The real impedance (Z') is given by $(\Delta E/\Delta I)\cos\phi$, and the imaginary impedance (Z") by $(\Delta E/\Delta I)\sin\phi$, where $\Delta E$ and $\Delta I$ are the amplitudes of the voltage and current modulation and $\phi$ is the phase shift. By plotting Z" *vs.* Z' as a function of the modulation frequency, one can obtain an impedance spectrum. The relation between a system's frequency response or impedance spectrum and stability is the Nyquist stability criterion. Detailed advantages and examples of the EIS technique will be explained in Chapter 2 (section 2.1.2). In its most rigorous and formal form, the Nyquist criterion is not particularly enlightening or easy to use, as it makes use of the theory of complex functions and conformal mappings. I prefer a simpler test which is entirely equivalent and which is based on the fact that it is very easy and intuitively clear to recognise the possibility of bifurcations from an impedance spectrum.

Recall that a bifurcation is a transition point where the system changes qualitatively from one type to the other. Linear stability analysis predicts that, at a bifurcation, small perturbations do not die out or grow. Hence, the solution of the linearised equations must be a sine wave, of finite frequency in the case of a Hopf bifurcation, and of $\omega_H$ zero frequency in the case of a saddle-node bifurcation. If the system is driven externally by a sine wave of exactly that critical frequency, a condition of resonance is encountered for which, in the ideal, linear case, the driving signal is blown up by the system without any phase delay. Hence, a bifurcation is a situation for which the impedance spectrum intersects the origin of the complex impedance plane. If the intersection occurs for non-zero frequency, the system exhibits a Hopf bifurcation; if the impedance spectrum terminates in the origin for zero frequency, the system exhibits a saddle-node bifurcation.

An impedance spectrum is measurable only if the system is stable. It is at this point that the role of the external circuit must be invoked. The majority of electrochemical oscillators lose their stability due to ohmic losses in the external circuit. Since the influence of an external ohmic resistance on the impedance spectrum amounts to a simple horizontal shift in the complex impedance plane, it is easy to test graphically for the possibility of a Hopf or saddle-node bifurcation from the impedance spectrum measured potentiostatically in the absence of an appreciable external ohmic drop or with the potentiostatic automatic IR compensation turned on. This test includes galvanostatic control, since this situation corresponds ideally to an infinite series resistance and an infinite applied potential, with their ratio equalling the fixed applied current. Hence, one must have infinitely negative real impedance and zero imaginary impedance in order to have a bifurcation under galvanostatic control, which is equivalent to zero real and imaginary admittance.

To summarise, we have the following conditions for detecting bifurcations from impedance characteristics with Z denoting impedance. For a fixed applied potential (one may call this potentiostatic, provided it is realised that there must be a sizable ohmic drop), an electrochemical cell will exhibit:

A saddle-node bifurcation if $Z(\omega) = 0,\ \omega = 0.$ (1.1)

A Hopf bifurcation if $Z(\omega) = 0,\ \omega = \omega_H \neq 0.$ (1.2)

**Negative impedance**

Assuming a linear potential drop inside the electrolyte under potentiostatic control, the load relation is given by $I = U/R - \phi/R$ where U is the applied constant potential and R denotes the uncompensated ohmic resistance. As long as the polarisation curve $I_{far}(\phi)$ is a monotonous function of the double layer potential (see Figure 1.1(a)), there is only one steady state for all values of U and R. In contrast, if $I_{far}$ exhibits a potential region of negative slope (Figures 1.1(b) and 1.1(c)), there are values of U and R for which the dynamics exhibits two stable states on branches of positive slope and one unstable state on the middle branch (bistability, see Figure. 1.1(c)). Since the slope of the polarisation curve is related to the sign of the electrochemical impedance (differential resistance), it follows that a negative impedance characteristics in combination with a sufficiently large ohmic resistance R are necessary for temporal bistability [29, 30]. For spontaneous potentiostatic oscillations of I and $\phi$ to occur (constantly applied potential U), an additional essential dynamical variable has to be considered aside from the double layer potential $\phi$. In the simplest case, the volume concentration, *c*, of a reactive chemical species near the interface can be taken into account resulting in an additional mass balance relation for *c*. Unlike the electrical variables, *c* is generally a slowly changing variable governed by the mass transfer from the bulk and the faradaic process decreasing *c*. Figure 1.1(d) sketches out the phase space representation of a periodic orbit: the N-shaped curve and the straight line denote the stationary $c-\phi$ values of the charge balance and mass balance, respectively. Again, the steady state marked by the intersection on the branch of negative impedance is unstable, driving the system to relax on the N-shaped manifold. If the system is on the active branch of low values of $\phi$ (high faradaic currents), the faradaic processes gradually consume the active species, decreasing $c$, and the operation point moves along the N-shaped curve toward smaller $c$.

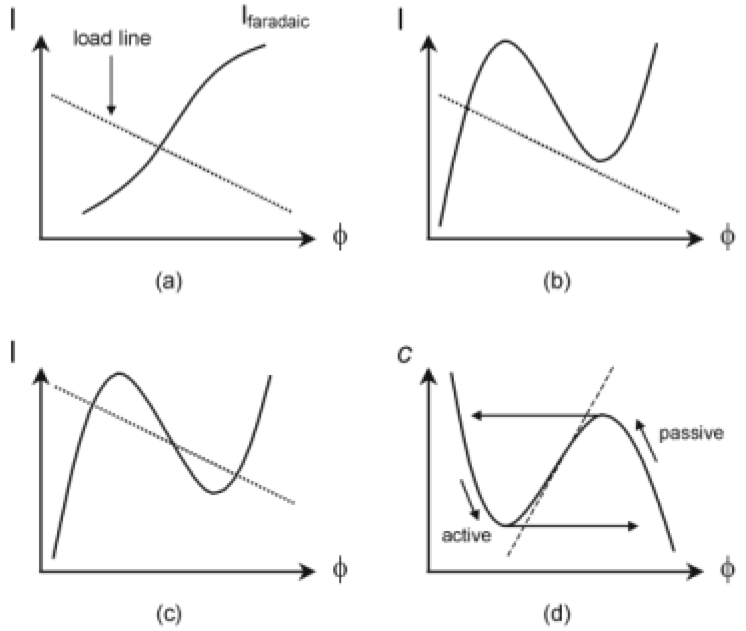

Figure 1.1. Schematic illustration of the origin of electrochemical instabilities: (a) single stationary state (mono-stability) with load line $I = U/R - \phi/R$ and monotonous faradaic $I - \phi$ profile; (b) single stationary state with N-shaped faradaic characteristic; (c) three stationary states (bistability) at suitable values of U and R; and (d) relaxation oscillations in an electrochemical two-variable system. The arrows indicate the trajectory of the periodic orbit within the $c - \phi$ phase space.

As the system reaches the extreme of the N-shaped curve, the system can not help but relax to the passive branch (low faradaic current). As $\phi$ is a very fast variable, this relaxation occurs very rapidly. The small current implies low rates of faradaic processes allowing for $c$ to replenish by diffusion. This, in turn, moves the system up along the N-shaped curve in Figure 1.1(c) until the system relaxes back to its initial state concluding a periodic cycle. One can show that it is (i) the negative impedance (negative differential resistance, NDR), (ii) a sufficiently large ohmic resistance and (iii) a properly balanced difference in time scales between electrical and chemical variables that is crucial for the occurrence of spontaneous potentiostatic oscillations of the type outlined. The chemical origin of negative impedance can be manifold. Typical examples in electrocatalytic reaction systems involve Frumkin-type double layer effects or the fast electrosorption of catalytically active or poisoning surface species. In these electrochemical oscillators, the negative impedance is visible by an N-shaped current-potential polarisation curve with the Hopf bifurcation located on the branch with negative impedance. Due to their simple mechanistic requirements, the outlined potentiostatic oscillations have been observed in a large number of experimental systems such as oxidations of cations, reduction of anions and electrocrystallisations [30, 31].

### Electrical double layer

The solution side of the double layer is thought to be made up of several **layers**. The closest one to the electrode, the inner layer, contains solvent molecules and some times other species (ions or molecules) that are said to be specifically adsorbed (Figure 1.2).

This inner layer is also called the compact, Helmholtz, or Stern layer. The locus of the electrical contents of the specifically adsorbed ions is called the inner Helmholtz plane (IHP), which is at a distance $x_1$. The total charge density from specifically adsorbed ions in this inner layer is $\sigma^{i}$ ($\mu$C/cm$^2$). Solvated ions can approach the metal only to a distance $x_2$; the locus of centres of these nearest solvated ions is called the outer Helmholtz plane (OHP). The interaction of the solvated ions with the charged metal involves only long-range electrostatic forces, so that their interaction is essentially independent of the chemical properties of the ions. These ions are non-specifically adsorbed. Due to thermal agitation in the solution, the non-specifically adsorbed ions are distributed in a three-dimensional region called the diffuse layer, which extends from the OHP into the bulk of the solution. The excess charge density in the diffuse layer is $\sigma^{d}$, hence the total excess charge density on the solution side of the double layer, $\sigma^{S}$, is given by

$$\sigma^{S} = \sigma^{i} + \sigma^{d} = -\sigma^{M}. \tag{1.3}$$

The structure of the double layer can affect the rates of electron processes. One usually cannot neglect the existence of the double layer capacitance or the presence of a charging current in electrochemical experiments. Indeed, during electrode reactions involving very low concentrations of electroactive species, the charging current can be much larger than the faradaic current for the reduction or oxidation reaction.

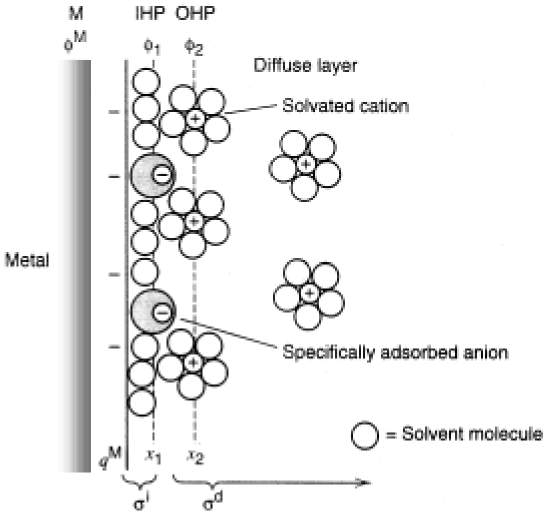

Figure 1.2. Proposed model of the double layer region under conditions where anions are specifically adsorbed [32].

### Coupling function in electrochemical systems

The kinetic description of an electrified interface considered exclusively spatially homogeneous systems, *i.e.*, systems in which any spatial potential variation was neglected. However, in the early 1900s, Ostwald [3] and Franck [7] assumed that the electrified interface is spatially inhomogeneous. Thus, spatial transport processes occurred parallel to the reactive interface and a spatial coupling term is needed to develop a correct model. Figure 1.3 shows the most common types of spatial coupling. A global coupling (see Figure 1.3(a)) is defined as one that is felt instantaneously and equally strongly at any spatial position of the system (electrode). A local coupling (Figure 1.3(b)) implies that only two points in close distance are coupled, while two distant points do not affect each other at all. Finally, a nonlocal coupling (see Figure 1.3(c)) is intermediately global and local in the sense that the region of coupling is wider than in the local case, possibly including the entire system, and that the coupling strength between two points varies with their spatial distance. Note that all spatial points along the electrode are assumed to be subject to the same coupling function in Figure 1.3. Recent relevant theoretical simulations [27] for specific electrode geometries such as ring and ribbon indicate that this is not necessarily the case. Both local coupling (*e.g.*, diffusion) and global coupling (*e.g.*, through the gas phase experiments under ultra high vacuum (UHV) conditions) have been extensively studied theoretically and experimentally [27].

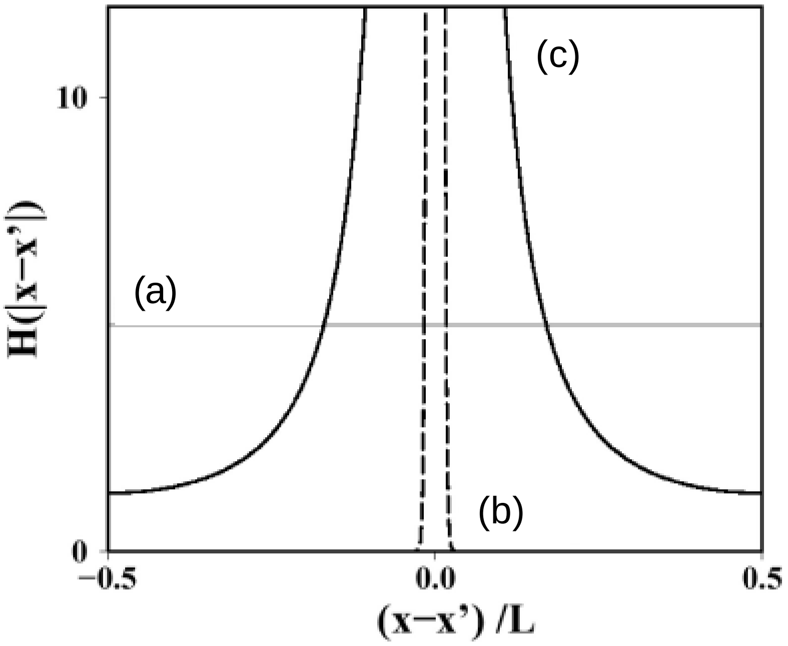

Figure 1.3. Common types of one-dimensional spatial coupling in dynamical systems with periodic boundary conditions. H denotes the coupling strength, (x – x') represents the spatial position relative to a reference point x'. Courtesy of J. Christoph [27].

Unlike reaction-diffusion systems in which spatiotemporal patterns result from the interaction of an autocatalysis and diffusion coupling, an additional transport mechanism occurs through the transport of charged species in an electric potential gradient (*e.g.*, migration processes) in electrochemical systems. The strong tendency of migration to neutralise net charge within the solution supports the assumption that the potential distribution can be governed by the Laplace equation rather than by the Poisson equation. This hypothesis is actually the starting point of all recent modelling approaches of spatial electrochemical pattern formation.

Previous modelling [12, 33] supported complex spatial patterns such as waves and anti-phase oscillations in the dissolution of Ni in $H_2SO_4$ solution. Even though there was a correspondence of the theoretical model and experimental data, the theoretical results were not quite clear due to unreasonable assumptions.

The model presented by Koper [34] could not allow for a nonlinear distribution of potential between the working electrode and the reference electrode, and potential inhomogeneities outside the diffusion layer were neglected, which is not in agreement with experimental observations [35]. Therefore, the latter model approach is also not able to adequately capture the characteristic of electrochemical coupling. Recently, Flätgen [36, 37] *et al.* reported on spatiotemporal patterns of the bistable and/or oscillatory phenomena in an NDR oscillator during the reduction of peroxodisulphate at a silver ring electrode. They observed travelling fronts along the electrode under bistable conditions (*i.e.*, the transition from active to passive states and *vice versa*). Interestingly, these fronts were accelerated, unlike the fronts with constant velocity to be occurred in reaction-diffusion systems.

Every electrochemical reaction produces charges that balance very quickly because no net charges can be built up in the electrolyte. The electroneutrality condition requires that for every surface element of the double layer, the capacitive and faradaic (reaction) currents ($i_{cap}$ and $i_{reac}$, respectively) be balanced by the migration current ($i_{mig}$) according to Kirchhoff’s law (the sum of the inflowing currents at a junction must be equal to the sum of outflowing currents).

$$i_{cap} = - i_{reac} + i_{mig}. \qquad (1.4)$$

Recently, Flätgen calculated the migration term ($i_{mig}$), *i.e.*, the potential gradient at the interface in direction of z, in the charge balance equation by solving the Laplace equation in two space dimensions x and z by means of Fourier modes, corresponding to parallel and perpendicular to the electrode, respectively. This equation governs the time evolution of the interfacial potential and therefore is the crucial part of the model.

$$C_{dl} \frac{\partial f_0(x, t)}{\partial t} = - I_{reac} + I_{mig} = - I_{far}(x, t) - \frac{s}{ß} \frac{\partial f\ (x, t)}{\partial z}\bigg|_{IF}, \qquad (1.5)$$

where $C_{dl}$ denotes the double layer capacity, $\beta$ is a geometrical parameter and $\sigma$ is the conductivity of the solution. This model clearly demonstrated the accelerated fronts, since there is nonlocal coupling across the electrolyte induced by migration currents parallel to the electrode.

Of late, J. Christoph [27] suggested an alternative approach to the calculation of the total migration current ($i_{mig}$) in the charge balance equation. He developed a numerically tractable formation for Eq. (1.5) by using **Green's functions**. Unlike several previous electrochemical models, his simulation led to illustrative integral representations of Eq. (1.5). In the case of periodic boundary conditions along the interface of a **ring** electrode with a rotationally symmetric point-like reference electrode, Eq. (1.5) can be written as

$$C_{dl}\frac{\partial f_0(x,t)}{\partial t} = F_{local}(x,t) + \int_0^{2\pi} H(|x - x'|)(\varphi'_0 - \varphi_0)\,dx', \qquad (1.6)$$

where the spatial coupling is entirely taken care of by the integral expression containing the coupling function $H$ and the potential difference of two points ($\varphi'_0 - \varphi_0$) considered. $F_{local}(x,t)$ indicates all local chemical dynamics. At the heart of the spatial integral coupling lies the spatial coupling function $H(|x - x'|)$, which represents the coupling between two points x and x' along the ring electrode. Due to the symmetry of the electrode geometry (ring), $H$ is simply a function of the distance $x - x'$ between two points. Spatial coupling along the WE occurs *via* ion migration in the electric field and is described by a coupling function $H$ (x, x'), which couples every location of the electrode to every other one.

Eq. (1.6) allows the precise formulation of three-dimensional ring geometry and it can also be used to approach complex geometries such as ribbon (see Chapter 5) or disc electrodes. Especially, for the geometry of interest for forthcoming experiments in Chapter 4 (*i.e.*, periodic boundary conditions in $x$ direction along a quasi one-dimensional WE with point RE on the rotational axis), the dependence of $H$ on system constraints such as (i) the geometric aspect ratio $\beta$ of the system (see section 4.6) and (ii) an external ohmic resistance $R_{ex}$ in series to the working electrode (see section 4.3) can be simplified as a single parameter B:

$$H = H(\mathrm{B}), \qquad \mathrm{B} = \mathrm{B}\,(\text{aspect ratio, } R_{ex}).$$

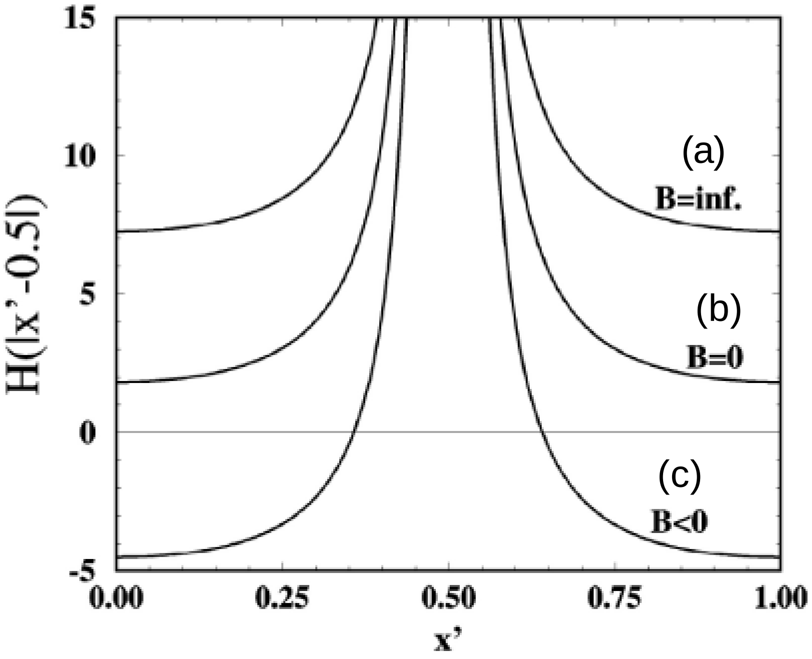

Figure 1.4. Dependence of the coupling function *H* on parameter B for a reference point located at x = 0.5. For large aspect ratios and no external resistance (*i.e.*, B = 0), *H* represents a positive nonlocal coupling. For small aspect ratios and no external resistance, B is negative. This gives rise to a positive short-range and negative long-range coupling. An additional external resistance increase B, which leads to a positive offset of H until in the galvanostatic limit (B = inf.) a strong positive nonlocal coupling exists. Courtesy of J. Christoph [27].

Figure 1.4 summarises the predictions of the integral formalism as to the dependence of the sign of *H* on the system parameter B. The system length was normalised to 1 and the reference point considered is located at x = 0.5. For a large distance of the reference electrode B is zero and the *H* is given by the middle curve (see (b)) in Figure 1.4. All points along the ring are coupled positively with coupling strength decreasing with distance. If the reference is approached towards the centre of the ring working electrode, B becomes negative; this leads to a negative offset of *H* resulting in a negative nonlocal coupling along the ring electrode, *i.e.*, a positive short-range and negative long-range coupling (see Figure 1.4(c)). The negative nonlocal coupling has important consequences as to the dynamical behaviour of the system. Two adjacent points along the ring tend to synchronise, while two distant points tend to be anticorrelated. Unlike a negative global coupling, the nonlocality of the negative coupling confines the opposite coupling to a more localised portion of the electrode. If an external resistance is set in series with the working electrode, the value of B increases, leading to a positive offset of the coupling function as marked with (a) in Figure 1.4. In the galvanostatic limit a strong positive nonlocal coupling results which instantaneously tends to synchronise the electrode. The negative nonlocal character of $H$ can give rise to qualitatively new dynamical states and phenomena unknown in reaction-diffusion systems. In Chapter 4 (ring) and Chapter 5 (ribbon-shaped electrode), experimental observations will support the theoretical predictions calculated by Christoph using the integral formalism [27].

## 1.3 Goal and outline

Fuel cell research has now established a fairly detailed picture of the chemistry involved in the electrocatalytic oxidations of $C_1$ fuels such as carbon monoxide (CO), formic acid (HCOOH) and methanol ($CH_3OH$) on noble metal electrodes [38 – 44].

A remarkable feature of the electrocatalytic oxidation reactions of organic $C_1$ fuels is the tendency for self-organised spatiotemporal instabilities at higher overpotentials or current loads [21, 22, 38, 40, 45 – 58]. Dynamical instabilities in electrochemistry most frequently arise through the interplay of the outer electrical load line and a sequence of faradaic processes with a non-monotonous current-potential characteristic [29, 30, 59]. More important in this work are non-stationary operation points in which the measured currents or potentials temporally exhibit sustained periodic behaviour, *i.e.*, autonomous electrochemical oscillations [30, 31]. Much work has been dedicated to clarification of the origin and the existence conditions of electrochemical oscillations in electro-oxidations of fuels [56, 57, 60 – 64]. Although long known, (*e.g.*, in the oxidation of formic acid [45, 46]) and despite its higher efficiency compared with stationary operations under certain conditions [65 – 68], oscillatory operation modes and a possible exploitation of periodic poisoning-activating processes received little attention in the context of energy conversion devices [40, 69].

The present work intends to contribute to our understanding of the electro-oxidation of $C_1$ molecules. It starts with the relatively simple CO oxidation, and moves on to formic acid and methanol, using both pure and modified electrode materials.

CO oxidation on platinum (Pt) and ruthenium (Ru)-modified Pt has been studied extensively before [42 – 44, 70], therefore Chapter 3 is restricted to pure Ru (in the form of smooth and rough Ru (0001)).

The mechanism of HCOOH oxidation on Pt is well established. Spatiotemporal pattern formation and the mechanistic origin of formic acid oxidation on a bismuth (Bi) deposited Pt ring electrode is the main subject of Chapter 4. Examples are standing waves, travelling pulse and autonomous/controlled pulse reversal. Then, in Chapter 5, another geometry, ribbon-shaped, is treated using a few representative examples of patterns. A ribbon-shaped Pt electrode was used in order to experimentally study the effects of edges, which manifest themselves in the stationary potential distribution as well as in in-phase and anti-phase edge oscillations on the ribbon. Chapter 6 concentrates on kinetic instabilities in methanol oxidation on Pt and Ru-modified Pt electrodes. Finally, a summary and outlook is given in Chapter 7.